Atmos. Chem. Phys. Discuss., 7, 9319–9365, 2007
www.atmos-chem-phys-discuss.net/7/9319/2007/

Atmospheric Chemistry and Physics Discussions

Intercomparison of ILAS-II Version 1.4 and Version 2 target parameters with MIPAS-Envisat measurements

A. Griesfeller[1,*], T. von Clarmann[2], J. Griesfeller[1,*], M. Höpfner[2], M. Milz[2], H. Nakajima[1], T. Steck[2], T. Sugita[1], T. Tanaka[1], and T. Yokota[1]

[1]National Institute for Environmental Studies (NIES), Tsukuba, Japan
[2]Institute of Meteorology and Climate Research (IMK-ASF), Forschungszentrum Karlsruhe and University Karlsruhe, Karlsruhe, Germany
[*]on leave

Received: 21 May 2007 – Accepted: 18 June 2007 – Published: 2 July 2007

Correspondence to: T. Sugita (tsugita@nies.go.jp)

Abstract

We compared measurements taken by two satellite-borne instruments, ILAS-II and MIPAS-Envisat, between May and October 2003. Using the coincidence criteria of ±300 km in space and ±12 h in time for H_2O, N_2O, and CH_4 and the coincidence criteria of ±300 km in space and ±6 h in time for $ClONO_2$, O_3, and HNO_3, a different number of coincidences have been found for the gases. The data were separated into sunrise and sunset measurements, which correspond to Northern and Southern Hemisphere data, respectively. For the sunrise data of ILAS-II, a clear improvement from Version 1.4 to Version 2.1 was observed for H_2O, CH_4, $ClONO_2$, and O_3. For ILAS-II N_2O and HNO_3 data there were no large differences between the two data sets. In particular, the ILAS-II Version 1.4 data were unrealistically small for H_2O, CH_4, and O_3 and unrealistically large for $ClONO_2$ above 20 km to 30 km. The differences between the two algorithm versions for the sunset data were not as large as for the sunrise data for all gases, and for H_2O and CH_4. ILAS-II Version 1.4 data fitted even better to the MIPAS-Envisat measurements than Version 2.0.

1 Introduction

Water vapor (H_2O), nitrous oxide (N_2O), methane (CH_4), ozone (O_3), nitric acid (HNO_3), and chlorine nitrate ($ClONO_2$) are trace species that play important roles in global warming, the greenhouse effect, and ozone-depletion processes in the lower stratosphere. As the most effective greenhouse gas in the troposphere, H_2O is responsible for about 65% of the natural greenhouse effect. H_2O is highly variable both in space and in time, so it is quite complicated to derive its influence on climate and chemistry. In particular, the amount of water vapor in the stratosphere has some effect on global warming (Forster and Shine, 1999). In the stratosphere, significant changes have been observed during the last four decades (Nedoluha et al., 1998). As a long-lived and vertically stratified species, N_2O is a useful tracer in dynamical studies (World

ACPD

7, 9319–9365, 2007

Meteorological Organization, 2003). It is also a greenhouse gas with a much larger specific effect on global warming than CO_2. Like N_2O, CH_4 is a tropospheric greenhouse gas, but it is not as long lived as N_2O (World Meteorological Organization, 2003). Its influence on global warming is larger than that of N_2O. O_3 is a stratospheric gas, with 90% of its column amount in the stratosphere and only 10% in the troposphere, that absorbs UV radiation in the stratosphere, keeping this radiation from reaching the Earth. Observing the vertical profile of O_3 is important for several reasons, including monitoring O_3 loss in the polar vortex (Bevilacqua et al., 1997; Singleton et al., 2005). Another key species in stratospheric ozone chemistry is HNO_3, a main nitrogen oxide reservoir gas, which determines the chemical and physical properties of the polar stratospheric clouds (PSCs) that play a central role in stratospheric ozone depletion (Solomon, 1999; World Meteorological Organization, 2003). $ClONO_2$ is a long-lived stratospheric chlorine reservoir species which plays an important role in the ozone loss chemistry with heterogeneous reactions on the surface on polar stratospheric clouds (Solomon, 1999).

The Advanced Earth Observing Satellite-II (ADEOS-II) with the Improved Limb Atmospheric Spectrometer-II (ILAS-II) was launched on H-IIA Launch Vehicle Flight No. 4 from Tanegashima Space Center at 10:31 a.m. on 14 December 2002 (Japanese Standard Time).

The polar-orbiting environmental satellite Envisat (Envisat = **ENVI**ronmental **SAT**ellite), which was launched on the night of 28 February 2002, in Kourou (French Guiana) on board an Ariane 5, carries ten instruments on board. Envisat is the largest satellite developed by the European Space Agency (ESA) to date. One of these ten instruments is the remote sensing instrument for atmospheric chemistry Michelson Interferometer for Passive Atmospheric Sounding (MIPAS) (Fischer, 1992, 1993; Fischer and Oelhaf, 1996).

This study investigates the differences between the vertical profiles derived from the data of MIPAS-Envisat and ILAS-II between May and October 2003. Measurement results were compared and differences were investigated in detail. The comparison

with the ILAS-II Version 1.4 and Version 2 data involved the retrieved data based on spectra version V3O (ESA: IPF 4.61/4.62) of a scientific data processor, developed at the Institute of Meteorology and Climate Research, Karlsruhe, Germany (IMK) (von Clarmann et al., 2003a,b), in cooperation with the Instituto de Astrofísica de Andalucía (IAA) in Granada, Spain (Funke et al., 2001).

2 Measurements and data analysis

2.1 ILAS-II

The ILAS-II solar occultation instrument was developed by the Ministry of the Environment (MOE) of Japan to succeed the ILAS. It was operated onboard the Advanced Earth Observing Satellite-II (ADEOS-II) spacecraft of the National Space Development Agency (NASDA) of Japan (recently restructured to become the Japan Aerospace Exploration Agency (JAXA)) (Nakajima et al., 2006) during its sun-synchronous polar orbit at an inclination angle of 98.7° and a height of 802.9 km. Measurements were made approximately 14 times daily in each hemisphere from January to October 2003. Latitudinal coverage was from 54°–71° N and 64°–88° S, varying seasonally. The instantaneous field of view (IFOV) for the infrared (IR) spectrometer at the tangent point was 1.0 km in the vertical and 13.0 km in the horizontal. ILAS-II included four observation channels. Three of them measured in the IR (850–1610 cm^{-1}, 1754–3333 cm^{-1}, and 778–782 cm^{-1}), and one in the visible (VIS, 12 755–13 280 cm^{-1}). ILAS-II used a solar occultation technique to measure stratospheric vertical profiles of O_3, HNO_3, NO_2, N_2O, CH_4, H_2O, $ClONO_2$, N_2O_5, CFC-11, CFC-12, and aerosol extinction coefficients. Vertical VMR profiles of atmospheric constituents are derived with an onion-peeling retrieval method (Yokota et al., 2002). The retrieval vertical grid interval was 1 km. Vertical resolutions were 1.3–2.9 km at tangent heights of 15 to 55 km (Nakajima et al., 2006). ILAS-II functioned continuously from April to October 2003 with some sporadic measurements between January and March 2003. Data obtained using the Version 1.4

retrieval algorithm have been validated by other independent measurements (Ejiri et al., 2006; Irie et al., 2006; Saitoh et al., 2006; Sugita et al., 2006). Further details about ILAS-II have been reported by Nakajima et al. (2006). ILAS-II measured absorption over a large spectral range. The gases examined in this paper were measured with Channel 1 at wavelengths from 850 to 1610 cm^{-1} with 44 spectral elements. There are many differences between ILAS-II Version 1.4 and Version 2. The most important change for the Northern Hemisphere data was the improvement of transmittance correction in the Northern Hemisphere: solar heat energy caused a distortion in the entrance slit, which resulted in abnormal transmittance. This was corrected only for the Northern Hemisphere data, because the transmittance distortion apparently appeared only for sunrise occultation events. Other major differences between ILAS-II Version 1.4 and Version 2 are the use of the HITRAN 2004 (Rothman et al., 2005) line parameters instead of HITRAN 2000 (Rothman et al., 2003) and the improvement of tangent height registration.

2.2 MIPAS-Envisat

MIPAS-Envisat (Fischer, 1992; Fischer and Oelhaf, 1996; Fischer et al., 2000) was developed at the ESA. It is a limb emission spectrometer that takes measurements of CH_4, ClO, $ClONO_2$, CO, CFC-11, CFC-12, H_2O, HNO_3, HNO_4, HOCl, N_2O_5, N_2O, NO_2, NO, O_3, and further trace gases in the infrared between 4 μm and 15 μm (2410 cm^{-1} and 685 cm^{-1}) with a spectral resolution of 0.035 cm^{-1} (unapodized) in five spectral bands, between 12 km and 68 km, performing 14.4 orbits per day. The orbit is sun synchronous in 800 km altitude with an inclination of 98.55°. The field of view is 30 km in the horizontal and 3 km in the vertical at the tangent points. While the operational ESA data are processed with a code described by Ridolfi et al. (2000), we used data from a science oriented data processor, developed at IMK in cooperation with IAA. The data used for comparison are based on calibrated radiance spectra generated by offline level-1 reprocessing and were labeled V3O. The scientific data processor uses the

ACPD
7, 9319–9365, 2007

Karlsruhe Optimized and Precise Radiative transfer Algorithm (KOPRA) as a forward model for the retrieval (Höpfner et al., 1998; Stiller et al., 1998; Stiller, 2000). MIPAS-Envisat took measurements nearly continuously from July 2002 until the end of March 2004. Instabilities in the interferometer driver velocity led to a temporary interruption of operational measurements at that point, but it was restarted with a different observation scheme in early 2005. Several MIPAS-Envisat data have already been validated, e.g. O_3 (Steck et al., 2007; Bracher et al., 2005; Verronen et al., 2005; Wang et al., 2005), N_2O (Bracher et al., 2005), HNO_3 (Wang et al., 2007), and $ClONO_2$ (Höpfner et al., 2007). However, these validation results are based partly upon different spectra, not only the spectra generated by offline level-1 reprocessing presented here. For MIPAS-Envisat the spectroscopy dataset of Flaud et al. (2003) is used. In contrast to the large spectral range in which the ILAS-II measurements were performed, the MIPAS-Envisat measurements used narrow wavelength bands called microwindows.

3 Results

Using the coincidence criteria of ±300 km in space and ±12 h in time for H_2O, N_2O, and CH_4 and the coincidence criteria of ±300 km in space and ±6 h in time for $ClONO_2$, O_3, and HNO_3, a different number of coincidences were found for these gases as shown in Tables 1 and 2 (see Sect. 3.2). The number of coincidences is different for each gas because MIPAS-Envisat data from the scientific data processor was not always available. Besides the number of coincidences, the average distance in space and time for the Northern and Southern Hemispheres are also listed in Tables 1 and 2 (see Sect. 3.2), respectively. These coincidence criteria were chosen to increase the number of coincidences and obtain more reliable statistics.

ACPD
7, 9319–9365, 2007

3.1 Northern Hemisphere

All Northern Hemisphere ILAS-II data considered here are sunrise data. The ILAS-II data are from the two retrieval algorithm Versions 1.4 and 2.1. The MIPAS-Envisat data of H_2O, $ClONO_2$, O_3, HNO_3, N_2O, and CH_4 are based on off-line spectra of Version 3 (V3O). In the Northern Hemisphere the measurements were made during summertime, so no polar vortex has to be considered. Measurements were performed between 54.8° N and 71.0° N (ILAS-II) and between 55.7° N and 72.4° N (MIPAS).

3.1.1 Water vapor

For the comparison of MIPAS-Envisat and ILAS-II H_2O data, we used Version V3O_H2O_11 of the scientific processor of MIPAS. The retrieval of the MIPAS-Envisat H_2O data has already been described in detail by Milz et al. (2005). Since the assumption of local thermodynamic equilibrium (LTE) is no longer valid above 50 km for the MIPAS-Envisat measurements, we compared only the data up to 50 km. In this comparison, we found 216 coincidences for the measurements in the Northern Hemisphere with most of the coincidences found from August until October (Fig. 1). For all months there was a clear improvement between the MIPAS-Envisat and the ILAS-II data from ILAS-II Version 1.4 in blue triangles to Version 2.1 in red circles.

Figure 2 shows the mean profiles of all coincidences along with the differences. The differences were calculated using the bias determination specification by von Clarmann (2006), the error bars represent the standard error of the mean difference. Obviously, the small values of ILAS-II Version 1.4 above 20 km were unrealistic. Up to 45 km there was good agreement between the MIPAS-Envisat measurements and the ILAS-II Version 2.1 data (except for the lowest data point). Above 45 to 50 km the values of the MIPAS-Envisat H_2O data were larger than the ILAS-II data. The largest differences were around 45 to 50 km with 2.6 ppmv (35%) for Version 2.1 data and 6.6 ppmv (85%) for Version 1.4.

ACPD
7, 9319–9365, 2007

EGU

3.1.2 Nitrous oxide

We used MIPAS-Envisat N_2O V3O_N2O_8 for comparison with the ILAS-II data. As was the case with H_2O, most of the coincidences we found between August and October (Fig. 3). In the five months from May until October there were 219 coincidences between MIPAS-Envisat and ILAS-II N_2O data. The retrieval of the MIPAS-Envisat N_2O and CH_4 data has already been described in detail by Glatthor et al. (2005).

For the tropospheric gas N_2O, the differences between the MIPAS-Envisat and the ILAS-II data were small (Fig. 4). There were also no large differences between the two retrieval versions of ILAS-II. Above 30 km the differences were small for both ILAS-II retrieval versions. The largest differences occured around 13 km and 14 km with values of 0.04 ppmv (12%) and 0.05 ppmv (14%) for ILAS-II Version 2.1 and Version 1.4, respectively. Mixing ratios measured by MIPAS-Envisat were found to be larger than the ILAS-II measurements for the whole height range.

3.1.3 Methane

For the comparison of MIPAS-Envisat and ILAS-II CH_4 data we used Version V3O_CH4_8 of the scientific processor of MIPAS. The coincidences were the same as for N_2O.

Similar to the case of H_2O, there was a clear improvement from ILAS-II Version 1.4 to ILAS-II Version 2.1. The small values of Version 1.4 above 25 km were unrealistic. Between MIPAS-Envisat and ILAS-II Version 2.1, the agreement was quite good. The largest differences, with 0.2 ppmv (14%), were at 22 km.

3.1.4 Ozone

The comparison of MIPAS-Envisat (V3O_O3_7) and ILAS-II O_3 data led to 118 coincident measurements in four months. The majority of these coincidences (59) were in October (Fig. 7), where there seemed to be two peaks between 25 km and 40 km.

ACPD
7, 9319–9365, 2007

For O_3 there was a slight improvement from ILAS-II Version 1.4 to ILAS-II Version 2.1, especially above 20 km. For the comparison with ILAS-II Version 2.1 data, the differences were about 0.3 ppmv (10%) for nearly the whole height range whereas above 20 km the differences with the ILAS-II Version 1.4 data increased, with the largest values of 0.85 ppmv (15%) being seen at 39 km.

3.1.5 Nitric acid

The coincidences we found for HNO_3 (V3O_HNO3_7) were the same as for O_3 (Fig. 9). The retrieval of the MIPAS-Envisat HNO_3 data has already been described in detail by Mengistu Tsidu et al. (2005). Wang et al. (2007) also compared HNO_3 data from MIPAS-Envisat and ILAS-II (only Version 1.4).

Figure 10 shows the differences between MIPAS-Envisat and ILAS-II measurements. The differences were quite small. The differences with ILAS-II Version 1.4 were slightly larger than with Version 2.1, especially above 20 km. The largest differences were around 25 km with 0.6 ppbv (7%) and 0.9 ppbv (10%) for Version 2.1 and Version 1.4, respectively. These differences were comparable to the differences found by Wang et al. (2007) for the ILAS-II Version 1.4 data. It is remarkable that, although in Version 2.1 the HITRAN 2004 line parameters were used instead of HITRAN 2000, no large differences were found, which might result from the fact that ILAS-II used not only the 11.3 μm band but also the 7.6 μm region for the retrieval, which compensates for the high bias of the 11.3 μm region (Wang et al., 2007).

3.1.6 Chlorine nitrate

For this comparison, the IMK Version V3O_ClONO2_11 was used. As in the case of H_2O and CH_4, there was a clear improvement in the ILAS-II $ClONO_2$ data from Version 1.4 to Version 2.1 above 30 km (Fig. 11). There was quite a good agreement between MIPAS-Envisat and ILAS-II Version 2.1. Below 25 km, there were large values of ILAS-II data for both versions of the ILAS-II retrieval algorithm. The retrieval of the

MIPAS-Envisat $ClONO_2$ data has already been described in detail by Höpfner et al. (2004, 2007).

Figure 12 shows the differences between the MIPAS-Envisat and ILAS-II data. For the Version 2.1 data, the differences (besides the lowest tangent altitude) were relatively small up to 30 km. Above 30 km the differences increased with largest differences of 0.13 ppbv (31%) at 35 km. For Version 1.4, the differences also were quite small below 30 km, but above that, the values were unrealistically large, resulting in very large differences with 0.6 ppbv (56%) around 37 km. This variation can be attributed to diurnal variation due to photochemistry (Höpfner et al., 2007).

3.2 Southern Hemisphere

All ILAS-II data taken in the Southern Hemisphere were sunset data. The ILAS-II data were from the two retrieval algorithm Versions 1.4 and 2.0. Measurements were performed between 68.5° S and 87.8° S (ILAS-II) and between 67.7° S and 86.6° S (MIPAS). The coincidences were separated into those from inside and those from outside the polar vortex using the criterion of Nash et al. (1996) at an equivalent latitude of 550 K. There were only six coincidences in May which were outside or at the edge of the polar vortex. All the other coincidences were clearly inside. The coincidences were listed in Table 2.

In the Southern Hemisphere there were no large differences between the two retrieval algorithms of ILAS-II. The differences between MIPAS-Envisat and the two ILAS-II retrieval versions are nearly the same. For H_2O and CH_4 ILAS-II Version 1.4 fits even better to the MIPAS-Envisat measurements than Version 2.0.

3.2.1 Water vapor

In the Southern Hemisphere 614 coincidences were found for H_2O and 608 of them were inside the polar vortex. In Fig. 13, it can be seen that there was no improvement between the two algorithm versions of ILAS-II. Above 45 km, the ILAS-II Version 1.4

data were slightly too large in comparison with the MIPAS-Envisat data.

The differences between MIPAS-Envisat and the two ILAS-II retrieval versions were not as large as for the Northern Hemisphere data (Fig. 14). This time the ILAS-II Version 1.4 agreed better with the MIPAS-Envisat data. The differences were about 1 to 2 ppmv (10 to 20% above 22 km) for nearly the whole altitude range, with smaller differences between MIPAS-Envisat and ILAS-II Version 1.4 data than with ILAS-II Version 2.0 data. Below 20 km, both instruments saw dehydrated air inside the polar vortex with very small VMR values of about 1 to 1.5 ppmv.

3.2.2 Nitrous oxide

Inside the polar vortex we found 568 coincidences between MIPAS-Envisat and ILAS-II measurements. Most of these coincidences (335) were in September (Fig. 15). There were no large differences between ILAS-II Version 1.4 and Version 2.0 data.

As N_2O is a tropospheric gas, the largest differences were obviously in the troposphere (Fig. 16). For this comparison the differences between the MIPAS-Envisat and ILAS-II measurements were quite small for the whole altitude range for both algorithm versions of ILAS-II. Especially above 20 km the differences were smaller than for the Northern Hemisphere data. The largest differences were around 13 km with 0.06 ppmv (21%) for Version 2.0 and 0.04 ppmv (14%) for Version 1.4. The MIPAS-Envisat measurements had larger values than the ILAS-II measurements for the whole height range for both hemispheres.

3.2.3 Methane

Figure 17 shows the comparison of ILAS-II Version 1.4 and Version 2.0 data with MIPAS-Envisat data. For the Southern Hemisphere data the agreement between the two retrieval versions of ILAS-II was much better, but in comparison with the Northern Hemisphere measurements, the differences between MIPAS-Envisat and ILAS-II Version 2 were larger than between MIPAS-Envisat and ILAS-II Version 1.4.

ACPD
7, 9319–9365, 2007

EGU

The differences are shown in Fig. 18. They were smaller than in the Northern Hemisphere, and the differences were especially small for ILAS-II Version 1.4. The largest differences for Version 2.0 were around 17 to 18 km with 0.26 ppmv (35%) and for Version 1.4 around 12 to 13 km with 0.12 ppmv (10%).

3.2.4 Ozone

MIPAS-Envisat and ILAS-II O_3 data had 218 coincidences in five months (Fig. 19).

In the Southern Hemisphere the differences between the two retrieval versions of ILAS-II were smaller, as was found with the other gases (Fig. 20). The largest differences were with 0.63 ppmv (17%) for Version 2.0 and 0.45 ppmv (12%) for Version 1.4 at around 27 to 28 km. Above 39 km, the differences between MIPAS-Envisat and ILAS-II Version 2.0 were smaller than between MIPAS-Envisat and ILAS-II Version 1.4. Below 39 km the situation was reversed.

3.2.5 Nitric acid

For the comparison of the southern hemispheric HNO_3 data inside the polar vortex, there were 227 coincidences (Fig. 21). Most of the coincidences were found in September. HNO_3 had a bi-modal distribution seen by both instruments in July 2003. In all other months there was only one mode. The large data in high altitudes in this bi-modal distribution were due to a high-altitude enhancement which was also seen by MIPAS-Envisat (Stiller et al., 2005). The low ILAS-II data for low altitudes were the result of denitrification.

Figure 22 shows the differences between the MIPAS-Envisat and the ILAS-II measurements. The differences were similar to the differences found in the Northern Hemisphere. For both retrieval versions the largest differences were at 25 km with 0.68 ppbv (10%) and 0.75 ppbv (10%) for Version 2.0 and Version 1.4, respectively. As was the case for the comparison of the Northern Hemisphere data, these differences were comparable to the differences found by Wang et al. (2007) for the ILAS-II Version 1.4

ACPD
7, 9319–9365, 2007

data.

3.2.6 Chlorine nitrate

In contrast to the measurements in the Northern Hemisphere there were no large differences between the two retrieval algorithms of ILAS-II in the Southern Hemisphere for $ClONO_2$ (Fig. 23). We found 199 coincidences between the MIPAS-Envisat and the ILAS-II measurements inside the polar vortex. Most of these coincidences were in September and October.

Figure 24 shows the differences between the MIPAS-Envisat and the ILAS-II data. The differences were relatively small for both retrieval versions of ILAS-II. The largest differences between MIPAS-Envisat and the ILAS-II Version 2.0 data were at 31 km with 0.19 ppbv (24%) and also at 31 km with 0.21 ppbv (27%) for ILAS-II Version 1.4.

4 Conclusions

The vertical VMR profiles of H_2O, N_2O, CH_4, O_3, HNO_3, and $ClONO_2$ were measured by MIPAS-Envisat and compared to profiles derived from ILAS-II measurements. We compared the measurements taken by these two instruments between May and October 2003. Using the coincidence criteria of ±300 km in space and ±12 h in time for H_2O, N_2O, and CH_4 and the coincidence criteria of ±300 km in space and ±6 h in time for $ClONO_2$, O_3, and HNO_3 a different number of coincidences was found for the gases. The data were separated into sunrise and sunset measurements, which correspond to Northern and Southern Hemisphere data, respectively. For the Northern Hemisphere data of H_2O, CH_4, $ClONO_2$, and O_3 from ILAS-II a clear improvement was observed from Version 1.4 to Version 2.1. For N_2O and HNO_3 data from ILAS-II there were no large differences observed. The differences between the two different algorithm versions for the Southern Hemisphere data were not as large as for the Northern Hemisphere data for all gases. Southern hemispheric H_2O and CH_4 profiles from ILAS-II

ACPD
7, 9319–9365, 2007

Version 1.4 fitted better than Version 2.0.

For the H_2O data, a clear improvement between the two retrieval versions of ILAS-II was noticed. The small values of ILAS-II Version 1.4 above 20 km in the Northern Hemisphere data were unrealistic. Up to 45 km there was good agreement between the MIPAS-Envisat measurements and the ILAS-II Version 2.1 data. Above 45 km, the MIPAS-Envisat values were too large. The largest differences between ILAS-II and MIPAS-Envisat H_2O data were around 45 to 50 km with 2.6 ppmv (35%) (Version 2.1) in the Northern Hemisphere and 1 to 2 ppmv (10 to 20% above 22 km) in the Southern Hemisphere (both Version 1.4 and Version 2.0). But compared to the Northern Hemisphere measurements, the differences between MIPAS-Envisat and ILAS-II Version 2 were larger than between MIPAS-Envisat and ILAS-II Version 1.4 in the Southern Hemisphere. For both H_2O and CH_4 there were unrealistically small values in Version 1.4 above 25 km in the Northern Hemisphere data. Between MIPAS-Envisat and ILAS-II Version 2.1, the agreement was quite good. The largest differences with 0.2 ppmv (14%) were at 22 km. In the Southern Hemisphere, the largest differences for Version 2.0 were at around 17 to 18 km with 0.26 ppmv (35%) and for Version 1.4 they were even smaller with 0.12 ppmv (10%) at around 12 to 13 km. O_3 showed only a slight improvement from ILAS-II Version 1.4 to ILAS-II Version 2.1 in the Northern Hemisphere. For the comparison with ILAS-II Version 2.1 data, the differences were of about 0.3 ppmv (10%), whereas above 20 km the differences with the ILAS-II Version 1.4 data increased with the largest values of 0.85 ppmv (15%) at 39 km. In the Southern Hemisphere the differences between the two retrieval versions of ILAS-II were smaller, with the largest differences of 0.63 ppmv (17%) for Version 2.0 and 0.45 ppmv (12%) for Version 1.4 at around 27 to 28 km. In the $ClONO_2$ data, the improvement in the Northern Hemisphere from ILAS-II Version 1.4 to ILAS-II Version 2.1 was again obvious because of the unrealistically large values of Version 1.4 data above 30 km. For the Version 2.1 data, the differences were relatively small up to 30 km. Above 30 km, the differences increased with largest differences of 0.13 ppbv (31%) at 35 km. In the Southern Hemisphere the differences were relatively small for both re-

ACPD
7, 9319–9365, 2007

EGU

trieval versions of ILAS-II, with the largest differences between MIPAS-Envisat and the ILAS-II Version 2.0 data being 0.19 ppbv (24%) and 0.21 ppbv (27%) for ILAS-II Version 1.4 both at 31 km. Both N_2O and HNO_3 data showed no large differences between the Version 1.4 and Version 2.1 in the Northern Hemisphere. The N_2O data showed the largest differences in the Northern Hemisphere around 13 and 14 km with values of 0.04 ppmv (12%) and 0.05 ppmv (14%) for ILAS-II Version 2.1 and Version 1.4, respectively, in the Southern Hemisphere at around 13 km with 0.06 ppmv (21%) for Version 2.0 and 0.04 ppmv (14%) for Version 1.4. The differences for HNO_3 were quite small with 0.6 ppbv (7%) and 0.9 ppbv (10%) for Version 2.1 and Version 1.4 around 25 km in the Northern Hemisphere and 0.68 ppbv (10%) and 0.75 ppbv (10%) for Version 2.0 and Version 1.4, respectively, in the Southern Hemisphere.

Acknowledgements. The ILAS-II project was funded by the Ministry of the Environment of Japan (MOE). A part of this research was supported by a Global Environment Research Fund (GERF) provided by the MOE.

References

Bevilacqua, R. M., Aellig, C. P., Debrestian, D., Fromm, M. D., Hoppel, K., Lumpe, J. D., Shettle, E. P., Hornstein, J. S., Randall, C. E., Rusch, D. W., and Rosenfield, J. E.: POAM II ozone observations in the Antarctic ozone hole in 1994, 1995 and 1996, J. Geophys. Res., 102, 23 643–23 658, 1997. 9321

Bracher, A., Bovensmann, H., Bramstedt, K., Burrows, J. P., von Clarmann, T., Eichmann, K.-U., Fischer, H., Funke, B., Gil-López, S., Glatthor, N., Grabowski, U., Höpfner, M., Kaufmann, M., Kellmann, S., Kiefer, M., Koukouli, M. E., Linden, A., López-Puertas, M., Mengistu Tsidu, G., Milz, M., Noël, S., Rohen, G., Rozanov, A., Rozanov, V. V., von Savigny, C., Sinnhuber, M., Skupin, J., Steck, T., Stiller, G. P., Wang, D.-Y., Weber, M., and Wuttke, M. W.: Cross comparisons of O_3 and NO_2 measured by the atmospheric ENVISAT instruments GOMOS, MIPAS, and SCIAMACHY, Adv. Space Res., 36, 855–867, doi:10.1016/j.asr.2005.04.005, 2005. 9324

Ejiri, M. K., Terao, Y., Sugita, T., Nakajima, H., Yokota, T., Toon, G. C., Sen, B., Wetzel, G.,

Oelhaf, H., Urban, J., Murtagh, D., Irie, H., Saitoh, N., Tanaka, T., Kanzawa, H., Shiotani, M., Kobayashi, H., and Sasano, Y.: Validation of the Improved Limb Atmospheric Spectrometer-II ILAS-II Version 1.4 nitrous oxide and methane profiles, J. Geophys. Res., 111, D22S90, doi:10.1029/2005JD006449, 2006. 9323

Fischer, H.: Remote sensing of atmospheric trace constituents using Fourier Transform Spectrometry, Ber. Bunsenges. Phys. Chem., 96, 306–314, 1992. 9321, 9323

Fischer, H.: Remote sensing of atmospheric trace gases, Interdisc. Sci. Rev., 18, 185–191, 1993. 9321

Fischer, H. and Oelhaf, H.: Remote sensing of vertical profiles of atmospheric trace constituents with MIPAS limb-emission spectrometers, Appl. Opt., 35, 2787–2796, 1996. 9321, 9323

Fischer, H., Blom, C., Oelhaf, H., Carli, B., Carlotti, M., Delbouille, L., Ehhalt, D., Flaud, J.-M., Isaksen, I., López-Puertas, M., McElroy, C. T., and Zander, R.: Envisat-MIPAS, an instrument for atmospheric chemistry and climate research, European Space Agency-Report SP-1229, edited by: Readings, C. and Harris, R. A., ESA Publications Division, ESTEC, P.O. Box 299, 2200 AG Noordwijk, The Netherlands, 2000. 9323

Flaud, J.-M., Piccolo, C., Carli, B., Perrin, A., Coudert, L. H., Teffo, J.-L., and Brown, L. R.: Molecular line parameters for the MIPAS (Michelson Interferometer for Passive Atmospheric Sounding) experiment, Atmos. Oceanic Opt., 16, 172–182, 2003. 9324

Forster, P. and Shine, K. P.: Stratospheric water vapor changes as a possible contributor to observed stratospheric cooling, Geophys. Res. Lett., 26, 3309–3312, 1999. 9320

Funke, B., López-Puertas, M., Stiller, G. P., von Clarmann, T., and Höpfner, M.: A new non–LTE Retrieval Method for Atmospheric Parameters From MIPAS–ENVISAT Emission Spectra, Adv. Space Res., 27, 1099–1104, 2001. 9322

Glatthor, N., von Clarmann, T., Fischer, H., Funke, B., Grabowski, U., Höpfner, M., Kellmann, S., Kiefer, M., Linden, A., Milz, M., Steck, T., Stiller, G. P., Mengistu Tsidu, G., and Wang, D. Y.: Mixing processes during the Antarctic vortex split in September/October 2002 as inferred from source gas and ozone distributions from ENVISAT-MIPAS, J. Atmos. Sci., 62, 787–800, 2005. 9326

Höpfner, M., Stiller, G. P., Kuntz, M., von Clarmann, T., Echle, G., Funke, B., Glatthor, N., Hase, F., Kemnitzer, H., and Zorn, S.: The Karlsruhe optimized and precise radiative transfer algorithm. Part II: Interface to retrieval applications, in: Optical Remote Sensing of the Atmosphere and Clouds, Beijing, China, 15–17 September 1998, edited by: Wang, J., Wu, B.,

Ogawa, T., and Guan, Z., vol. 3501, pp. 186–195, 1998. 9324
Höpfner, M., von Clarmann, T., Fischer, H., Glatthor, N., Grabowski, U., Kellmann, S., Kiefer, M., Linden, A., Mengistu Tsidu, G., Milz, M., Steck, T., Stiller, G. P., Wang, D.-Y., and Funke, B.: First spaceborne observations of Antarctic stratospheric $ClONO_2$ recovery: Austral spring 2002, J. Geophys. Res., 109, D11308, doi:10.1029/2004JD004609, 2004. 9328
Höpfner, M., von Clarmann, T., Fischer, H., Funke, B., Glatthor, N., Grabowski, U., Kellmann, S., Kiefer, M., Linden, A., Milz, M., Steck, T., Stiller, G. P., Bernath, P., Blom, C. E., Blumenstock, T., Boone, C., Chance, K., Coffey, M. T., Friedl-Vallon, F., Griffith, D., Hannigan, J. W., Hase, F., Jones, N., Jucks, K. W., Keim, C., Kleinert, A., Kouker, W., Liu, G. Y., Mahieu, E., Mellqvist, J., Mikuteit, S., Notholt, J., Oelhaf, H., Piesch, C., Reddmann, T., Ruhnke, R., Schneider, M., Strandberg, A., Toon, G., Walker, K. A., Warneke, T., Wetzel, G., Wood, S., and Zander, R.: Validation of MIPAS $ClONO_2$ measurements, Atmos. Chem. Phys., 7, 257–281, 2007, http://www.atmos-chem-phys.net/7/257/2007/. 9324, 9328
Irie, H., Sugita, T., Nakajima, H., Yokota, T., Oelhaf, H., Wetzel, G., Toon, G. C., Sen, B., Santee, M. L., Terao, Y., Saitoh, N., Ejiri, M. K., Tanaka, T., Kondo, Y., Kanzawa, H., Kobayashi, H., and Sasano, Y.: Validation of stratospheric nitric acid profiles observed by Improved Limb Atmospheric Spectrometer (ILAS)-II, J. Geophys. Res., 111, D11S03, doi:10.1029/2005JD006115, 2006. 9323
Mengistu Tsidu, G., Stiller, G. P., von Clarmann, T., Funke, B., Höpfner, M., Fischer, H., Glatthor, N., Grabowski, U., Kellmann, S., Kiefer, M., Linden, A., López-Puertas, M., Milz, M., Steck, T., and Wang, D. Y.: NO_y from Michelson Interferometer for Passive Atmospheric Sounding on Environmental Satellite during the Southern Hemisphere polar vortex split in September/October 2002, J. Geophys. Res., 110, D11301, doi:10.1029/2004JD005322, 2005. 9327
Milz, M., von Clarmann, T., Fischer, H., Glatthor, N., Grabowski, U., Hpfner, M., Kellmann, S., Kiefer, M., Linden, A., Mengistu Tsidu, G., Steck, T., Stiller, G. P., Funke, B., López-Puertas, M., and Koukouli, M. E.: Water Vapor Distributions Measured with the Michelson Interferometer for Passive Atmospheric Sounding on board Envisat (MIPAS/Envisat), J. Geophys. Res., 110, D24307, doi:10.1029/2005JD005973, 2005. 9325
Nakajima, H., Sugita, T., Yokota, T., Kobayashi, H., Sasano, Y., Ishigaki, T., Mogi, Y., Araki, N., Waragai, K., Kimura, N., Iwazawa, T., Kuze, A., Tanii, J., Kawasaki, H., Horikawa, M., Togami, T., and Uemura, N.: Characteristics and performance of the Improved Limb Atmospheric Spectrometer-II (ILAS-II) on board the ADEOS-II satellite, J. Geophys. Res., 111, D11S01, doi:10.1029/2005JD006334, 2006. 9322, 9323

Nash, E. R., Newman, P. A., Rosenfield, J. E., and Schoeberl, M. R.: An objective determination of the polar vortex using Ertel's potential vorticity, J. Geophys. Res., 101, 9471–9478, 1996. 9328

Nedoluha, G. E., Bevilacqua, R. M., Gomez, R. M., Siskind, D. E., Hicks, B. C., and Russell III, J. M.: Increases in middle atmospheric water vapor as observed by the Halogen Occultation Experiment (HALOE) and the ground-based Water Vapor Millimeter-wave Spectrometer from 1991 to 1997, J. Geophys. Res., 103, 3531–3542, 1998. 9320

Ridolfi, M., Carli, B., Carlotti, M., von Clarmann, T., Dinelli, B., Dudhia, A., Flaud, J.-M., Höpfner, M., Morris, P. E., Raspollini, P., Stiller, G., and Wells, R. J.: Optimized Forward and Retrieval Scheme for MIPAS Near-Real-Time Data Processing, Appl. Opt., 39, 1323–1340, 2000. 9323

Rothman, L. S., Barbe, A., Benner, D. C., Brown, L. R., Camy-Peyret, C., Carleer, M. R., Chance, K., Clerbaux, C., Dana, V., Devi, V. M., Fayt, A., Flaud, J.-M., Gamache, R. R., Goldman, A., Jacquemart, D., Jucks, K. W., Lafferty, W. J., Mandin, J.-Y., Massie, S. T., Nemtchinov, V., Newnham, D. A., Perrin, A., Rinsland, C. P., Schroeder, J., Smith, K. M., Smith, M. A. H., Tang, K., Toth, R. A., Auwera, J. V., Varanasi, P., and Yoshino, K.: The HITRAN Molecular Spectroscopic Database: Edition of 2000 Including Updates through 2001, HITRAN Special Issue: J. Quant. Spectrosc. Ra., 82, 5–44, 2003. 9323

Rothman, L. S., Jacquemart, D., Barbe, A., Benner, D. C., Birk, M., Brown, L. R., Carleer, M. R., Chackerian Jr., C., Chance, K., Coudert, L., Dana, V., Devi, V. M., Flaud, J.-M., Gamache, R. R., Goldman, A., Hartmann, J.-M., Jucks, K. W., Maki, A. G., Mandin, J.-Y., Massie, S. T., Orphal, J., Perrin, A., Rinsland, C. P., Smith, M. A. H., Tennyson, J., Tolchenov, R. N., Toth, R. A., Auwera, J. V., Varanasi, P., and Wagner, G.: The HITRAN 2004 Molecular Spectroscopic Database, HITRAN Special Issue: J. Quant. Spectrosc. Ra., 96, 139–204, 2005. 9323

Saitoh, N., Hayashida, S., Sugita, T., Nakajima, H., Yokota, T., Hayashi, M., Shiraishi, K., Kanzawa, H., Ejiri, M. K., Irie, H., Tanaka, T., Terao, Y., Kobayashi, H., and Sasano, Y.: Intercomparison of ILAS-II version 1.4 aerosol extinction coefficient at 780 nm with SAGE II, SAGE III, and POAM III, J. Geophys. Res., 111, D11S05, doi:10.1029/2005JD006315, 2006. 9323

Singleton, C. S., Randall, C. E., Chipperfield, M. P., Davies, S., Feng, W., Bevilacqua, R. M., Hoppel, K. W., Fromm, M. D., Manney, G. L., and Harvey, V. L.: 2002-2003 Arctic ozone loss deduced from POAM III satellite observations and the SLIMCAT chemical transport model,

Atmos. Chem. Phys., 5, 597–609, 2005, http://www.atmos-chem-phys.net/5/597/2005/. 9321

Solomon, S.: Stratospheric Ozone Depletion: A Review of Concepts and History, Rev. Geophys., 37, 275–315, 1999. 9321

Steck, T., von Clarmann, T., Fischer, H., Funke, B., Glatthor, N., Grabowski, U., Höpfner, M., Kellmann, S., Kiefer, M., Linden, A., Milz, M., Steck, T., Stiller, G. P., Wang, D. Y., Alaart, M., Blumenstock, T., von der Gathen, P., Hansen, G., Hase, F., Hochschild, G., G.Kopp, Kyrö, E., Oelhaf, H., Raffalski, U., Redondas Marrero, A., Remsberg, E., Russell III, J., Stebel, K., Steinbrecht, W., Wetzel, G., Yela, M., and Zhang, G.: Bias determination and precision validation of ozone profiles from MIPAS-Envisat retrieved with the IMK-IAA processor, Atmos. Chem. Phys. Discuss., 7, 4427–4480, 2007, http://www.atmos-chem-phys-discuss.net/7/4427/2007/. 9324

Stiller, G. P. (Ed.): The Karlsruhe Optimized and Precise Radiative Transfer Algorithm (KOPRA), Forschungszentrum Karlsruhe, Wissenschaftliche Berichte, FZKA 6487, 2000. 9324

Stiller, G. P., Höpfner, M., Kuntz, M., von Clarmann, T., Echle, G., Fischer, H., Funke, B., Glatthor, N., Hase, F., Kemnitzer, H., and Zorn, S.: The Karlsruhe optimized and precise radiative transfer algorithm. Part I: Requirements, justification, and model error estimation, in: Optical Remote Sensing of the Atmosphere and Clouds, Beijing, China, 15–17 September 1998, edited by: Wang, J., Wu, B., Ogawa, T., and Guan, Z., vol. 3501, pp. 257–268, 1998. 9324

Stiller, G. P., Mengistu Tsidu, G., von Clarmann, T., Glatthor, N., Höpfner, M., Kellmann, S., Linden, A., Ruhnke, R., Fischer, H., López-Puertas, M., Funke, B., and Gil-López, S.: An enhanced HNO_3 second maximum in the Antarctic mid–winter upper stratosphere 2003, J. Geophys. Res., 110, D20303, doi:10.1029/2005JD006011, 2005. 9330

Sugita, T., Nakajima, H., Yokota, T., Kanzawa, H., Gernandt, H., Herber, A., von der Gathen, P., Koenig-Langlo, G., Sato, K., Dorokhov, V., Yushukov, V. A., Murayama, Y., Yamamori, M., Godin-Beekmann, S., Goutail, F., Roscoe, H., Deshler, T., Yela, M., Taalas, P., Kyro, E., Oltmans, S., Johnson, B., Allaart, M., Litynska, Z., Klekociuk, A., Andersen, S. B., Braathen, G., De Backer, H., Randall, C. E., Thomason, L. W., Irie, H., Ejiri, M. K., Saitoh, N., Tanaka, T., Terao, Y., Kobayashi, H., and Sasano, Y.: Ozone profiles in the high-latitude stratosphere and lower mesosphere measured by the Improved Limb Atmospheric Spectrometer (ILAS)-II: Comparison with other satellite sensors and ozonesondes, J. Geophys. Res., 111, D11S02, doi:10.1029/2005JD006439, 2006. 9323

Verronen, P., Kyrölä, E., Funke, B., Gil-López, S., Kaufmann, M., López-Puertas, M., von Clarmann, T., Stiller, G., Grabowski, U., and Höpfner, M.: A Comparison of night-time GOMOS and MIPAS vertical ozone profiles in the stratosphere and mesosphere, Adv. Space Res., 36, 958–966, 2005. 9324

von Clarmann, T.: Validation of remotely sensed profiles of atmospheric state variables: strategies and terminology, Atmos. Chem. Phys., 6, 4311–4320, 2006, http://www.atmos-chem-phys.net/6/4311/2006/. 9325

von Clarmann, T., Chidiezie Chineke, T., Fischer, H., Funke, B., García-Comas, M., Gil-López, S., Glatthor, N., Grabowski, U., Höpfner, M., Kellmann, S., Kiefer, M., Linden, A., López-Puertas, M., López-Valverde, M. Á., Mengistu Tsidu, G., Milz, M., Steck, T., and Stiller, G. P.: Remote Sensing of the Middle Atmosphere with MIPAS, in: Remote Sensing of Clouds and the Atmosphere VII, edited by: Schäfer, K., Lado-Bordowsky, O., Comerón, A., and Picard, R. H., vol. 4882, pp. 172–183, SPIE, Bellingham, WA, USA, 2003a. 9322

von Clarmann, T., Glatthor, N., Grabowski, U., Höpfner, M., Kellmann, S., Kiefer, M., Linden, A., Mengistu Tsidu, G., Milz, M., Steck, T., Stiller, G. P., Wang, D. Y., Fischer, H., Funke, B., Gil-López, S., and López-Puertas, M.: Retrieval of temperature and tangent altitude pointing from limb emission spectra recorded from space by the Michelson Interferometer for Passive Atmospheric Sounding (MIPAS), J. Geophys. Res., 108, 4736, doi:10.1029/2003JD003602, 2003b. 9322

Wang, D.-Y., Stiller, G. P., von Clarmann, T., Fischer, H., Glatthor, N., Grabowski, U., Höpfner, M., Kellmann, S., Kiefer, M., Linden, A., Mengistu Tsidu, G., Milz, M., Steck, T., Wohnsiedler, S., López-Puertas, M., Funke, B., Gil-López, S., Kaufmann, M., Koukouli, M., Murtagh, D., Lautie, N., Jimenez, C., Jones, A., Eriksson, P., Urban, J., Noe, J., Flochmoen, E., Dupuy, E., Ricaud, P., Olberg, M., Frisk, U., Russel III, J., and Remsberg, E.: Comparisons of MIPAS/ENVISAT ozone profiles with SMR/ODIN and HALOE/UARS observations, Adv. Space Res., 36, 927–931, 2005. 9324

Wang, D. Y., Höpfner, M., Mengistu Tsidu, G., Stiller, G. P., von Clarmann, T., Fischer, H., Blumenstock, T., Glatthor, N., Grabowski, U., Hase, F., Kellmann, S., Linden, A., Milz, M., Oelhaf, H., Schneider, M., Steck, T., Wetzel, G., López-Puertas, M., Funke, B., Koukouli, M. E., Nakajima, H., Sugita, T., Irie, H., Urban, J., Murtagh, D., Santee, M. L., Toon, G., Gunson, M. R., Irion, F. W., Boone, C. D., Walker, K., and Bernath, P. F.: Validation of nitric acid retrieved by the IMK-IAA processor from MIPAS/ENVISAT measurements, Atmos. Chem. Phys., 7, 721–738, 2007,

http://www.atmos-chem-phys.net/7/721/2007/. 9324, 9327, 9330
World Meterorological Organization: Scientific Assessment of Ozone Depletion: 2002, Global Ozone Res. and Monit. Proj. Rep. No. 47, Geneva, 2003. 9320, 9321
Yokota, T., Nakajima, H., Sugita, T., Tsubaki, H., Itou, Y., Kaji, M., Suzuki, M., Kanzawa, H., Park, J. H., and Sasano, Y.: Improved Limb Atmospheric Spectrometer (ILAS) data retrieval algorithm for Version 5.20 gas profile products, J. Geophys. Res., 107, 8216, doi:10.1029/2001JD000628, 2002. 9322

Table 1. Coincidences of MIPAS-Envisat and ILAS-II measurements in the Northern Hemisphere.

Gas	# of coinc.	Average Δ space [km]	Average Δ lat. [°]	Average Δ long. [°]	Average Δ time [hours]
H_2O	216	168	−0.27	−1.37	6:11
		±84	±1.04	±3.05	±2:24
N_2O	219	168	−0.27	−1.35	6:11
		±83	±1.04	±3.04	±2:26
CH_4	219	168	−0.27	−1.35	6:11
		±83	±1.04	±3.04	±2:26
O_3	118	167	−0.29	−1.92	4:21
		±86	±1.05	±2.61	±1:21
HNO_3	118	167	−0.29	−1.92	4:21
		±86	±1.05	±2.61	±1:21
$ClONO_2$	118	167	−0.29	−1.92	4:21
		±86	±1.05	±2.61	±1:21

ACPD
7, 9319–9365, 2007

Table 2. Coincidences of MIPAS-Envisat and ILAS-II measurements in the Southern Hemisphere. The number in brackets indicate the number of coincidences inside the polar vortex.

Gas	# of coinc.	Average Δ space [km]	Average Δ lat. [°]	Average Δ long. [°]	Average Δ time [hours]
H_2O	614	189	0.20	0.06	7:22
	(608)	±68	±1.30	±17.52	±3:48
N_2O	574	188	0.21	0.01	7:25
	(568)	±68	±1.28	±17.78	±3:48
CH_4	574	188	0.21	0.01	7:25
	(568)	±68	±1.28	±17.78	±3:48
O_3	224	207	−0.06	−0.70	2:58
	(218)	±54	±1.44	±15.06	±1:33
HNO_3	233	209	−0.11	−0.38	2:58
	(227)	±54	±1.53	±15.34	±1:32
$ClONO_2$	205	211	−0.06	−0.60	3:01
	(199)	±54	±1.42	±15.19	±1:36

ACPD
7, 9319–9365, 2007

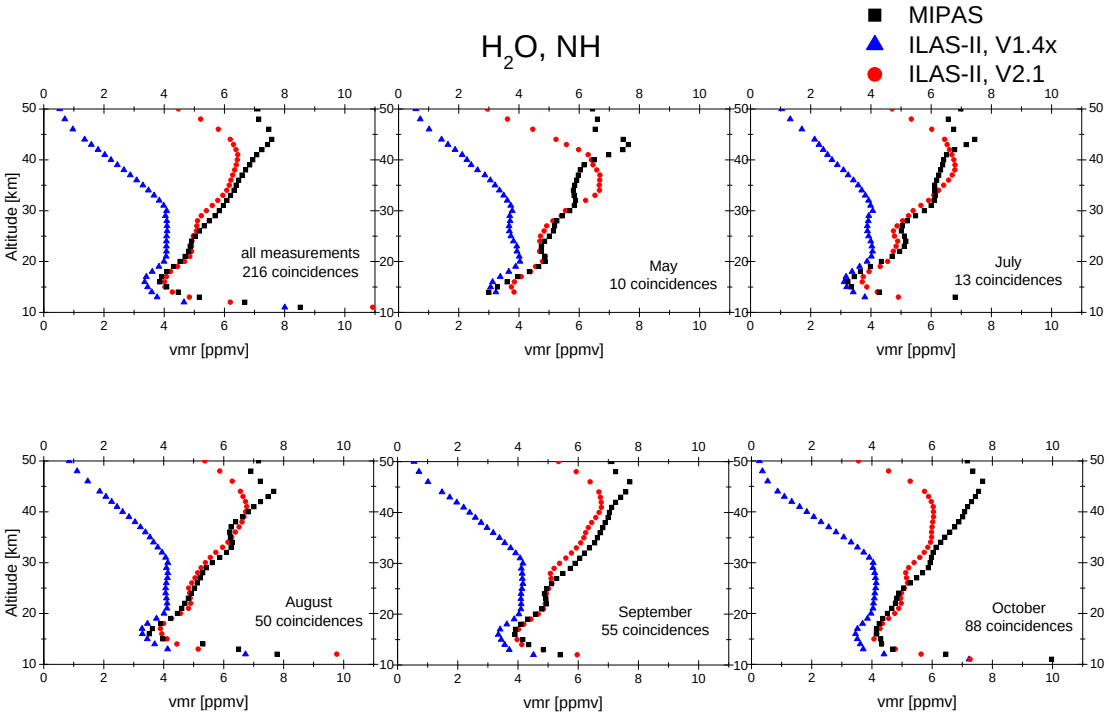

Fig. 1. Comparison of the H_2O measurements in the Northern Hemisphere. The mean profiles of the MIPAS-Envisat measurements are shown as black squares, the mean profiles of the ILAS-II V1.4 data as blue triangles and the mean profiles of the ILAS-II V2.1 data as red circles for each month we found coincidences.

ACPD
7, 9319–9365, 2007

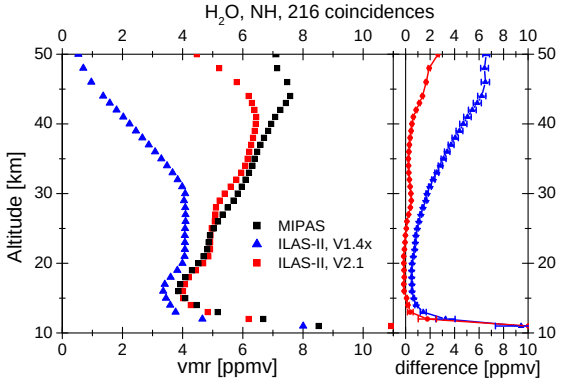

Fig. 2. Differences between MIPAS-Envisat and ILAS-II measurements of H_2O in the Northern Hemisphere. The mean profiles of all coincidences of the MIPAS-Envisat measurements are shown as black squares, the mean profiles of the ILAS-II V1.4 data as blue triangles and the mean profiles of the ILAS-II V2.1 data as red circles. At the right hand side the differences along with the standard error of the mean difference between the MIPAS-Envisat measurements and the ILAS-II V1.4 data are shown in blue and between the MIPAS-Envisat and the ILAS-II V2.1 data in red.

ACPD
7, 9319–9365, 2007

EGU

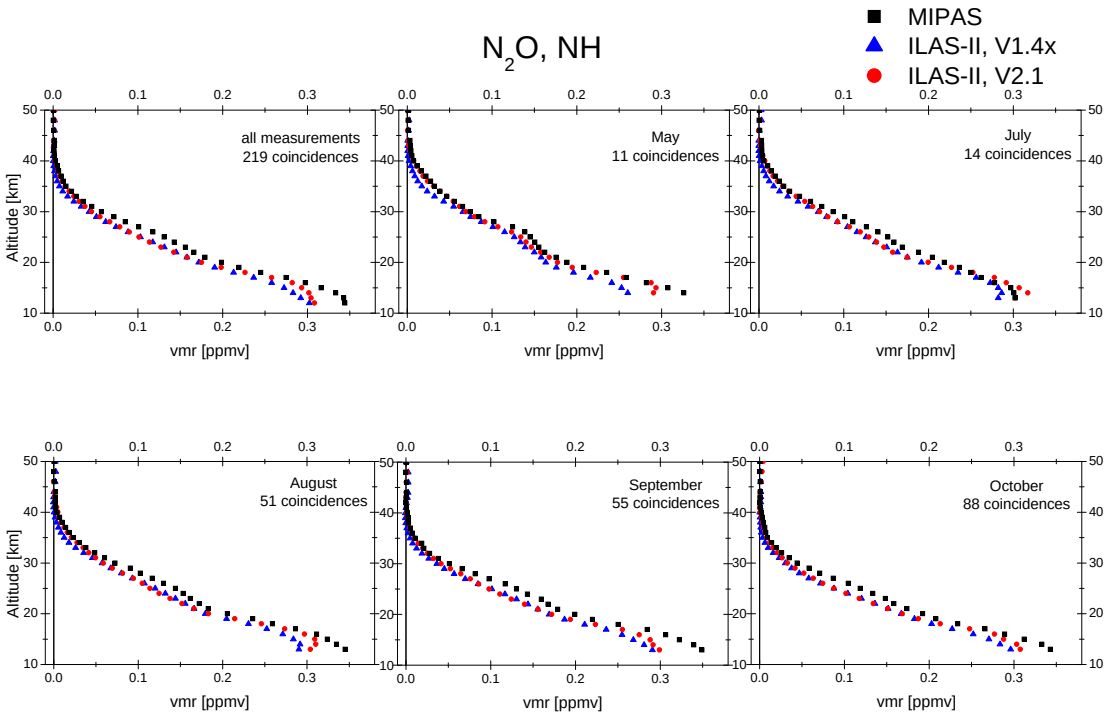

Fig. 3. As in Fig. 1 but for N_2O.

ACPD
7, 9319–9365, 2007

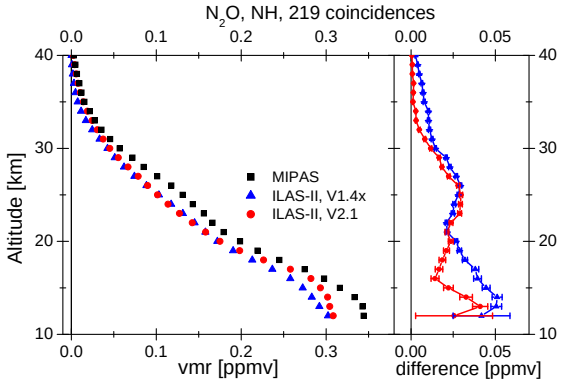

Fig. 4. As in Fig. 2 but for N_2O.

ACPD
7, 9319–9365, 2007

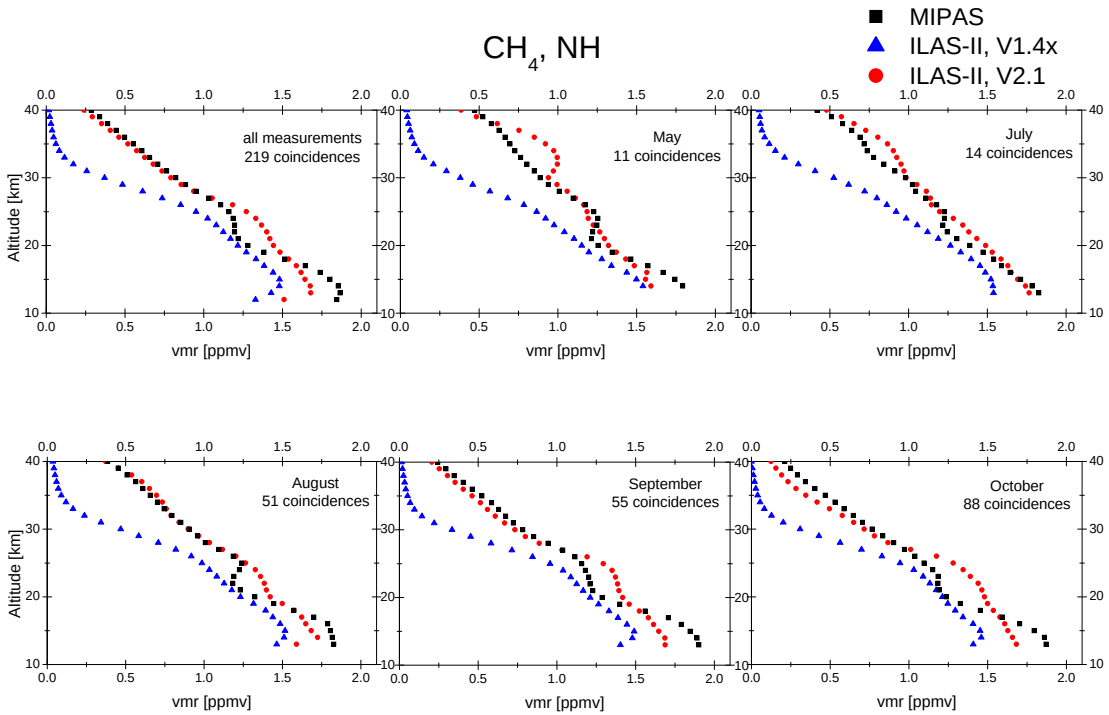

Fig. 5. As in Fig. 1 but for CH_4.

ACPD
7, 9319–9365, 2007

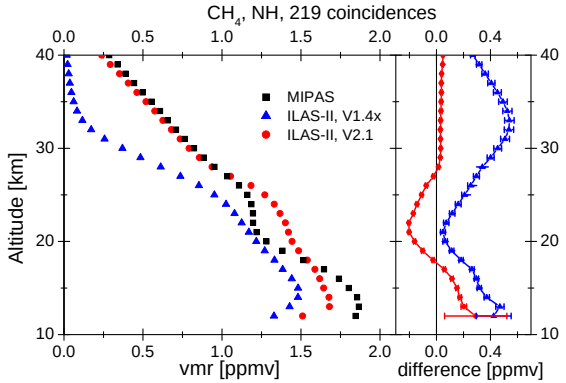

Fig. 6. As in Fig. 2 but for CH_4.

ACPD
7, 9319–9365, 2007

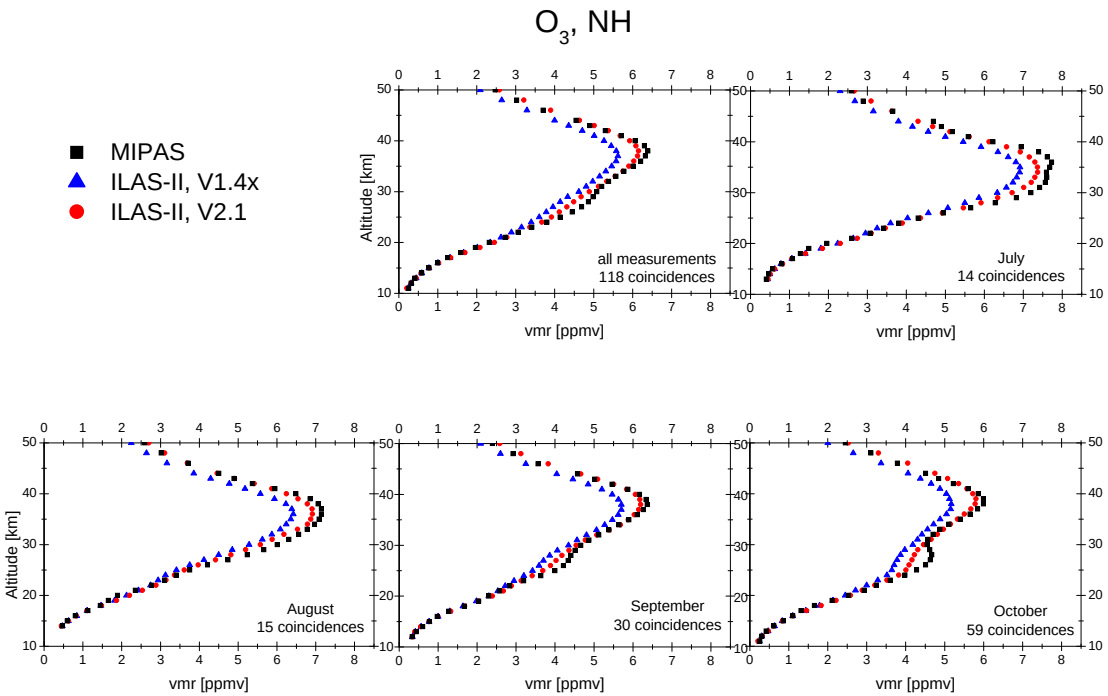

Fig. 7. As in Fig. 1 but for O_3.

ACPD
7, 9319–9365, 2007

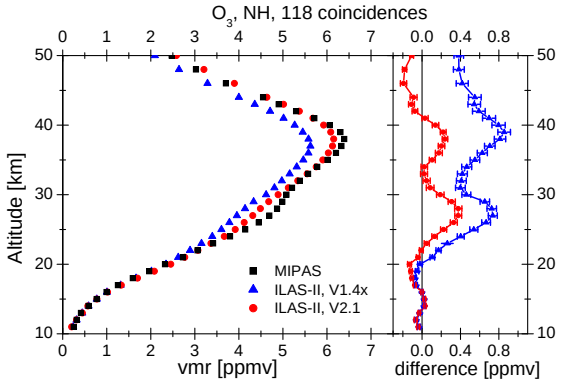

Fig. 8. As in Fig. 2 but for O_3.

ACPD
7, 9319–9365, 2007

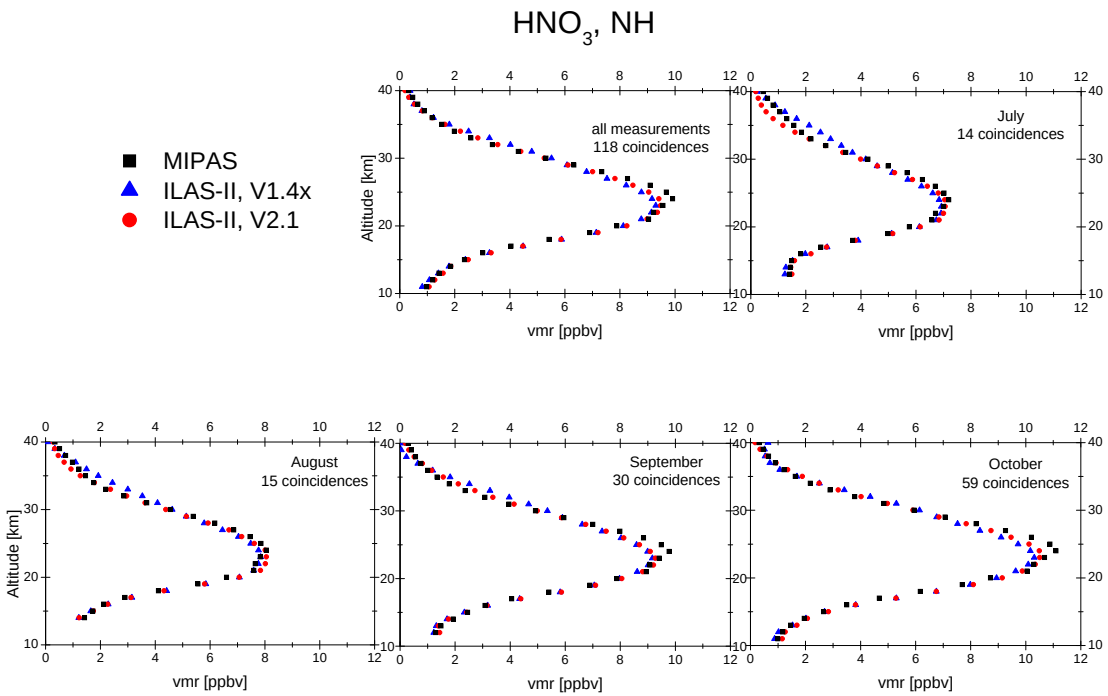

Fig. 9. As in Fig. 1 but for HNO_3.

ACPD
7, 9319–9365, 2007

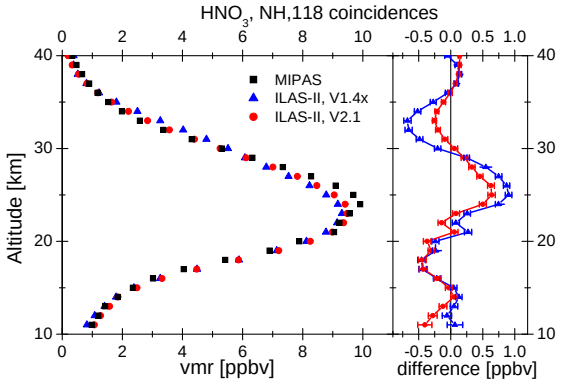

Fig. 10. As in Fig. 2 but for HNO_3.

ACPD
7, 9319–9365, 2007

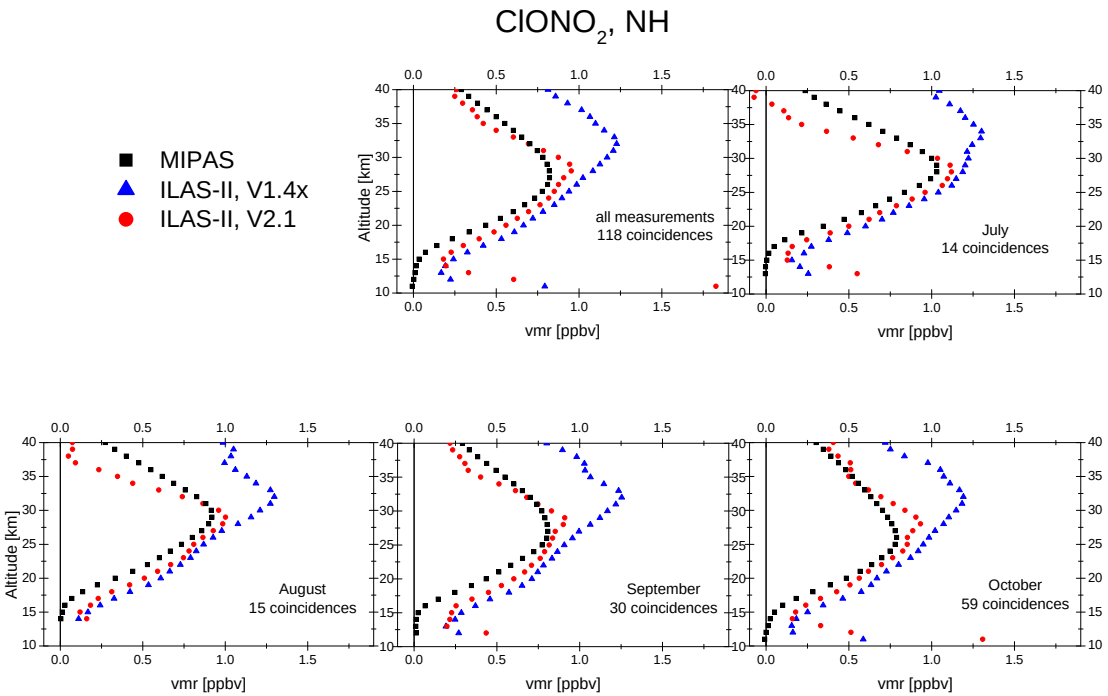

Fig. 11. As in Fig. 1 but for $ClONO_2$.

ACPD
7, 9319–9365, 2007

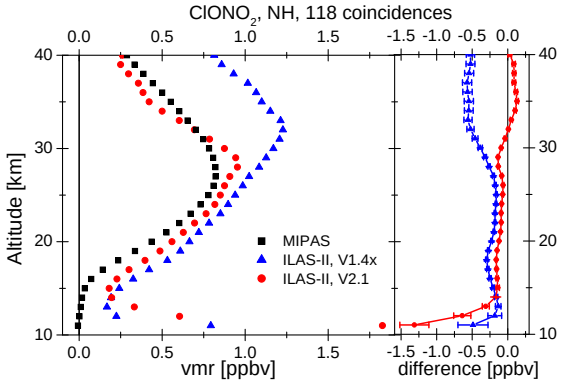

Fig. 12. As in Fig. 2 but for $ClONO_2$.

ACPD
7, 9319–9365, 2007

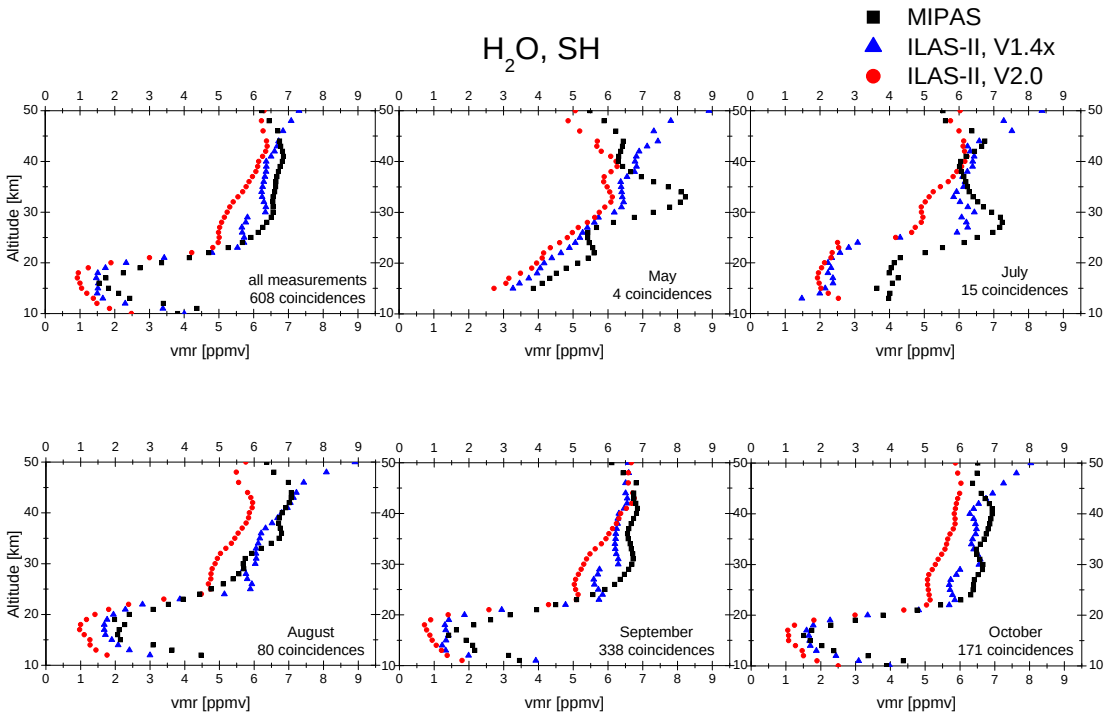

Fig. 13. Comparison of the H_2O measurements in the Southern Hemisphere. The MIPAS-Envisat measurements are shown as black squares, the ILAS-II V1.4 data as blue triangles and the ILAS-II V2.0 data as red circles for each month we found coincidences.

ACPD
7, 9319–9365, 2007

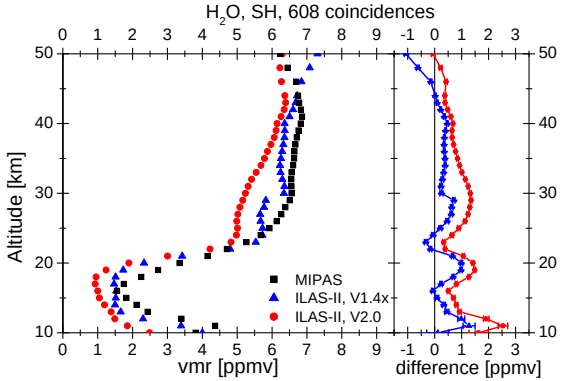

Fig. 14. Differences between MIPAS-Envisat and ILAS-II measurements of H_2O in the Southern Hemisphere. The mean profiles of all coincidences of the MIPAS-Envisat measurements are shown as black squares, the mean profiles of the ILAS-II V1.4 data as blue triangles and the mean profiles of the ILAS-II V2.0 data as red circles. At the right hand side the differences along with the standard error of the mean difference between the MIPAS-Envisat measurements and the ILAS-II V1.4 data are shown in blue and between the MIPAS-Envisat and the ILAS-II V2.0 data in red.

ACPD
7, 9319–9365, 2007

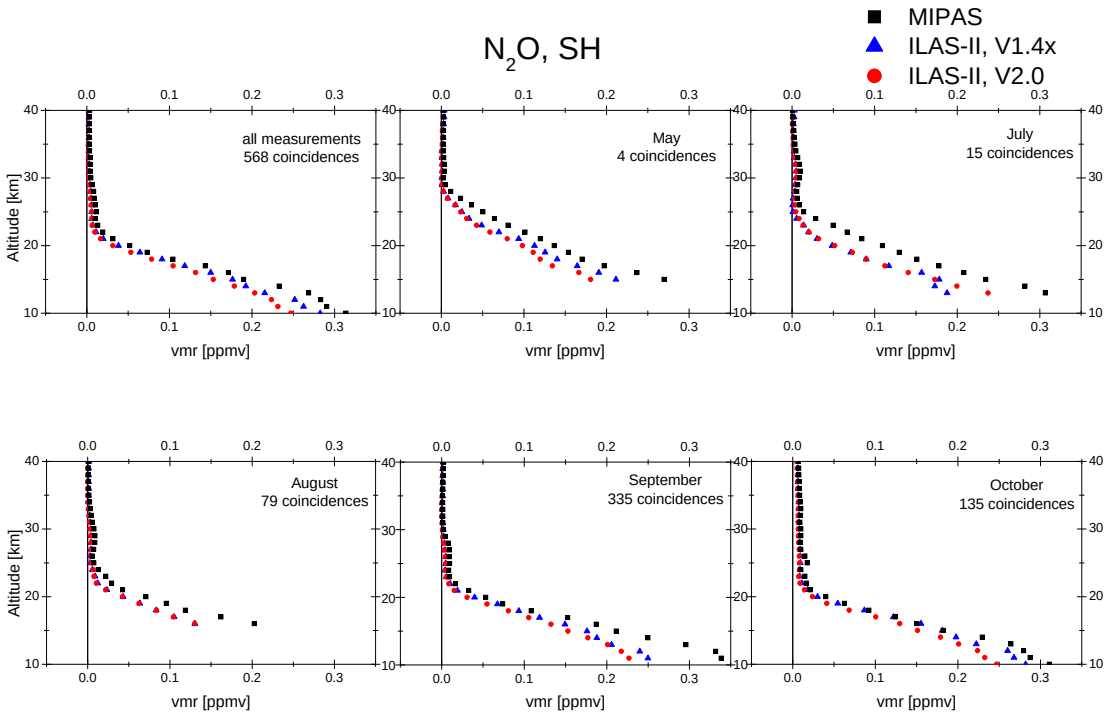

Fig. 15. As in Fig. 13 but for N_2O.

ACPD
7, 9319–9365, 2007

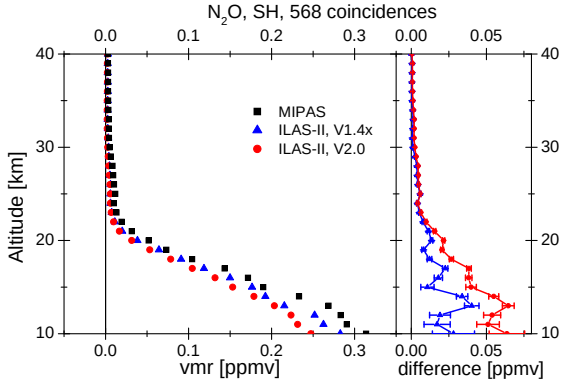

Fig. 16. As in Fig. 14 but for N_2O.

ACPD
7, 9319–9365, 2007

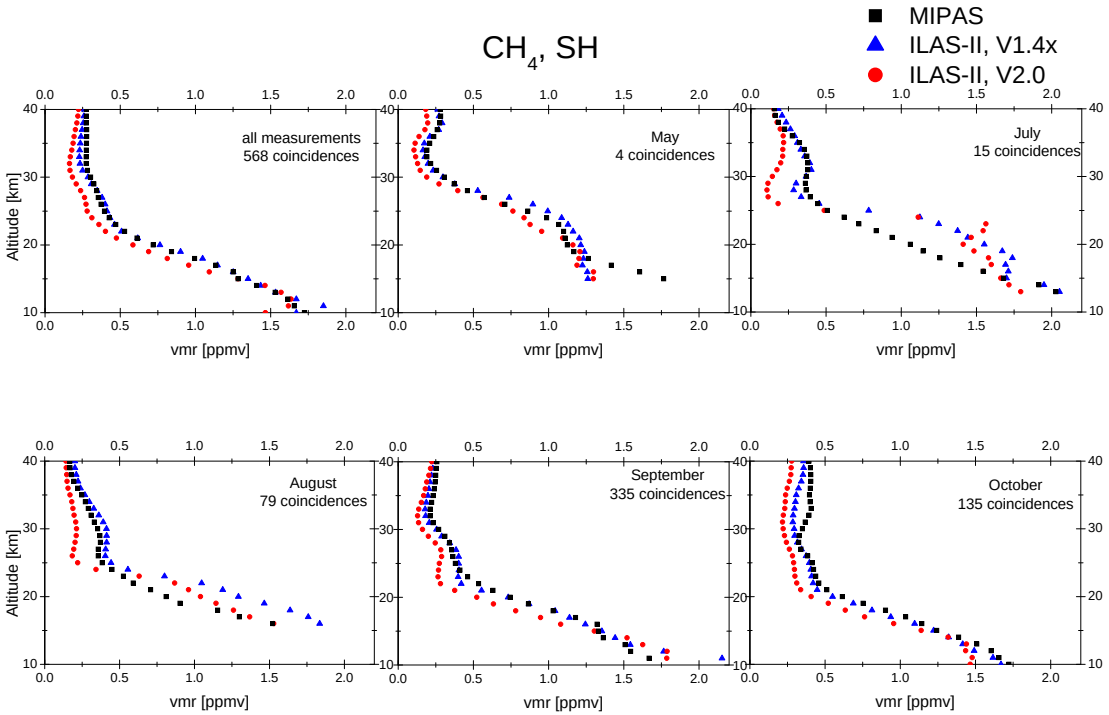

Fig. 17. As in Fig. 13 but for CH_4.

ACPD
7, 9319–9365, 2007

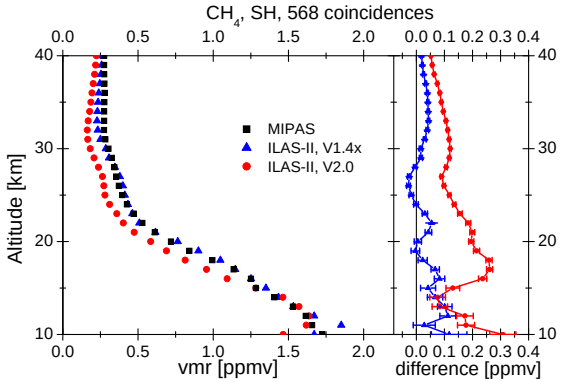

Fig. 18. As in Fig. 14 but for CH_4.

ACPD
7, 9319–9365, 2007

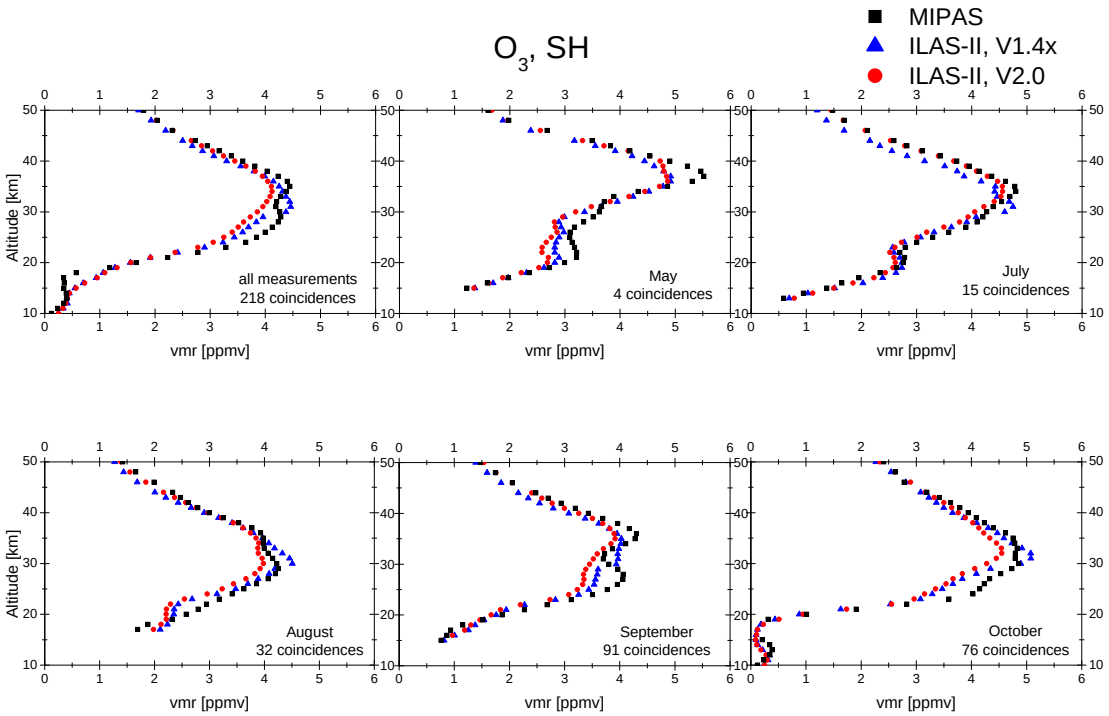

Fig. 19. As in Fig. 13 but for O_3.

ACPD
7, 9319–9365, 2007

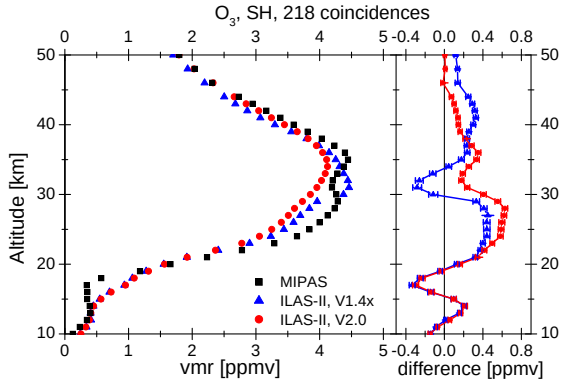

Fig. 20. As in Fig. 14 but for O_3.

ACPD
7, 9319–9365, 2007

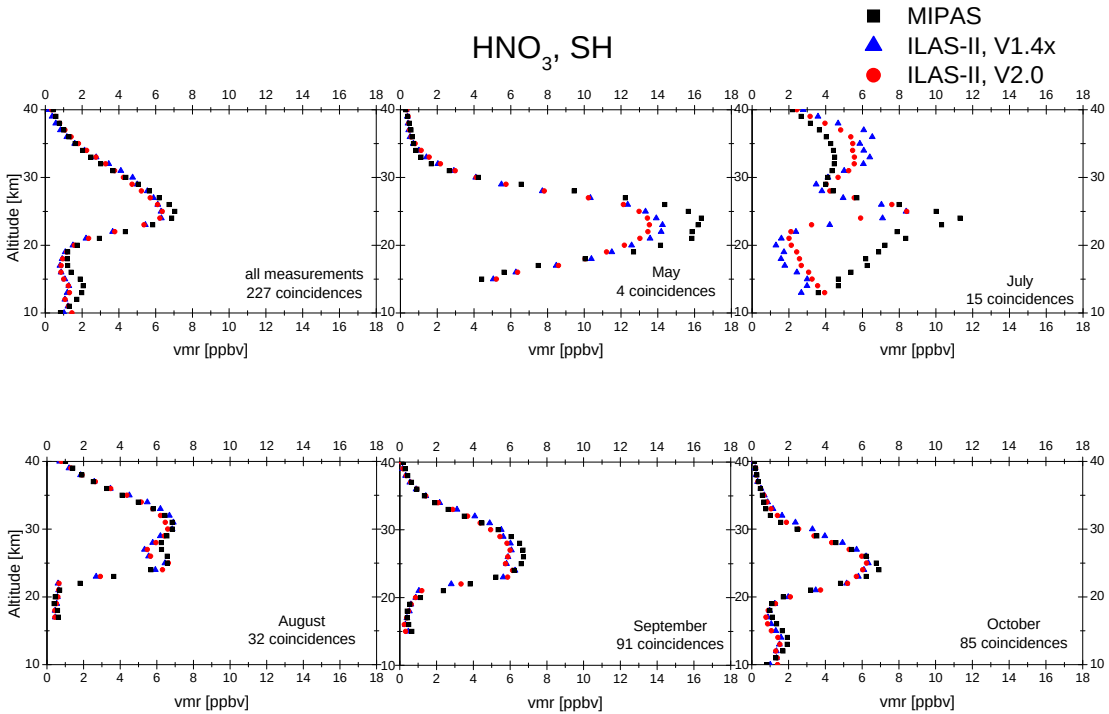

Fig. 21. As in Fig. 13 but for HNO_3.

ACPD
7, 9319–9365, 2007

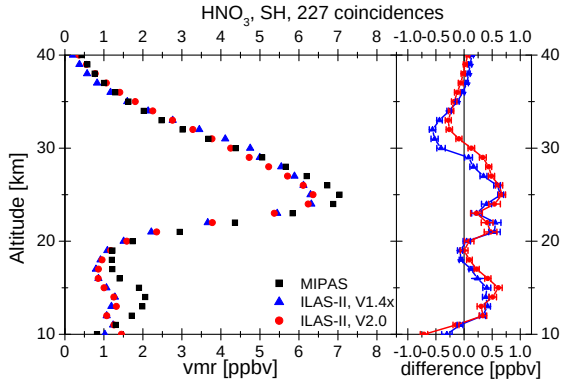

Fig. 22. As in Fig. 14 but for HNO_3.

ACPD
7, 9319–9365, 2007

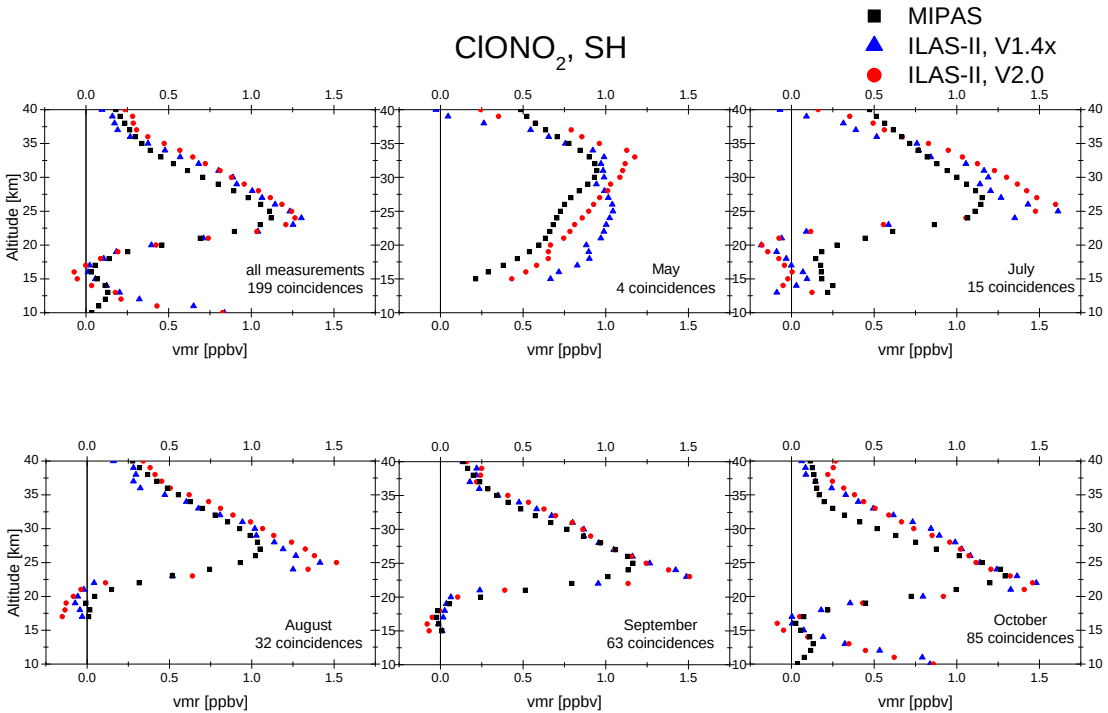

Fig. 23. As in Fig. 13 but for $ClONO_2$.

ACPD
7, 9319–9365, 2007

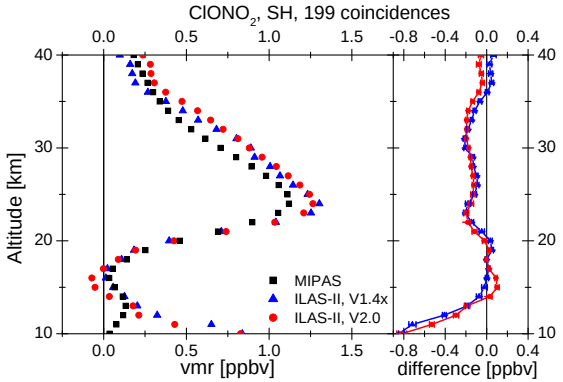

Fig. 24. As in Fig. 14 but for $ClONO_2$.

ACPD
7, 9319–9365, 2007